### **ABSTRACTS**

### **ISS Edinburgh 2014 Scientific Paper Presentations**

Published online: 12 June 2014

© ISS 2014

### Special Scientific Session (SSS) Program

ISS Edinburgh—Members Meeting
Tuesday, October 14, 2014, 1:30 PM—5:30 PM
Ad Hoc Scientific Session Committee:
Miriam Bredella, Juerg Hodler, Carrie Inwards, Christian Pfirrmann,
Kathryn Stevens, Martin Torriani. Chair: Jenny T. Bencardino.

### Session 1

**Moderators:** Juerg Hodler, Zurich, Switzerland and Martin Torriani, Boston, USA

1:30 PM. Assessment of pars interarticularis fractures using MRI with a 3D fat suppressed T1 weighted gradient echo sequence compared to CT

Peter Counsel, Angus Brown, Marcus Davenport, David A Connell, Paul Marks. Melbourne, Australia.

**Purpose:** To assess the accuracy of 3.0 T MRI including a 3D fat suppressed T1 weighted gradient-echo sequence (T1 High Resolution Isotropic Volume ExCitation, THRIVE) in diagnosis of pars fractures compared to CT.

**Materials and Methods:** A retrospective study of 48 patients, aged 11 to 28 (mean 17) who had undergone CT and MRI for a clinical query of pars fracture. The 190 pars in the field of the targeted CTs were analyzed by two readers with consensus.

**Results:** Using CT as the gold standard, there were 37 complete fractures, 31 incomplete fractures and 122 intact pars. MRI correctly identified 36 (97.3 %) complete fractures, with 1 (2.7 %) labeled incomplete. Of 31 incomplete fractures, 27 (87.1 %) were correctly called incomplete and 1 complete (3.2 %). The three (9.7 %) incomplete fractures that were not appreciated had no edema, and two of these had correctly identified acute abnormalities (one stress reaction, one incomplete fracture) of the contralateral pars. There were no false positive fractures.

**Conclusion:** A 3D fat suppressed T1 weighted gradient echo sequence is a valuable addition to MRI protocols investigating pars fractures, almost as accurate as CT, and may aid in reducing radiation exposure to this predominantly young group of patients.

# $1\!:\!40$ PM. MRI findings in the lumbar spines of asymptomatic elite junior tennis players

Gajan Rajeswaran, Michael Turner, Conor Gissane, Jeremiah C Healy. London, United Kingdom.

Purpose: To evaluate the MRI findings in the lumbar spines of asymptomatic elite junior tennis players.

**Materials and Methods:** The lumbar spine MRI studies of 98 asymptomatic junior elite tennis players (51 male, 47 female) with a mean age of 18 years was reviewed by 2 consultant musculoskeletal radiologists using consensus opinion using accepted classification systems.

Results: 4 players (4 %) had no abnormality. Facet joint arthropathy occurred in 89.7 % of the players. There were 41 synovial cysts all occurring in the presence of facet arthropathy. Disc degeneration was noted in 62.2 % of players. Disc herniation was noted in 30.6 % players with 86.1 % of being broad based and nerve root compression in 2 %. There were 41 pars interarticularis abnormalities with grade 1 spondylolisthesis in 5.1 % of players. The prevalence of facet joint arthropathy, disc degeneration, disc herniation and pars interarticularis fracture was lower in females than males and in the under 16 s than the over 20s.

**Conclusion:** There is a significant amount of underlying pathology that would normally go undetected in this group of asymptomatic elite athletes. The relevance of these findings is to facilitate appropriate rehabilitation to prevent loss of playing time and potentially career ending injuries.

1:50 PM. Finite element analysis applied to high-resolution 3 T MRI of proximal femur microarchitecture detects lower bone strength in subjects with fragility fractures compared to controls who do not differ by bone mineral density

Gregory Chang, Stephen Honig, Ryan Brown, Cem M Deniz, Kenneth Egol, James S. Babb, Ravinder R. Regatte, Chamith S. Rajapakse. New York, USA.

**Purpose:** To determine whether magnetic resonance imaging (MRI) assessment of bone strength on proximal femur microarchitecture images has added value as a biomarker of bone quality.

Materials and Methods: This study had institutional review board approval, and written informed consent was obtained. We recruited 22 post-menopausal women with fragility fractures and 22 matched controls without fracture. All subjects underwent dual-energy x-ray absorptiometry (DXA) and 3 T MRI of proximal femur microarchitecture using a new 26-element coil (same hip). On MR images, we applied finite element analysis to compute elastic modulus (measure of bone strength). We compared differences in BMD T-scores and elastic moduli between groups and assessed the relationship between elastic moduli and BMD T-scores.

**Results:** Fracture cases demonstrated lower elastic modulus compared to controls (p<0.05 for all: femoral head, 8.51–8.73 vs. 9.32–9.67 GPa; femoral neck, 3.11–3.72 vs. 4.39–4.82 GPa; Ward's Triangle, 1.85–2.21 vs. 3.98–4.13 GPa; intertrochanteric, 1.62–2.18 vs. 3.86–4.47 GPa; greater trochanter, 0.65–1.21 vs. 1.96–2.62 GPa), but no differences in BMD. There were weak relationships between elastic moduli and BMD in fracture cases (R2=0.25-0.31, p=0.02–0.04), but not in controls.

**Conclusion:** MRI assessment of proximal femur strength may provide information about bone quality that is not captured by DXA.



# 2:00 PM. FDG-PET avidity of breast and lung metastases to the proximal femur as a predictor of pathologic fracture

Tae Won B. Kim, Alexandra M. Zindman, John H. Healey New York, USA.

**Purpose:** Mirels rating system is traditionally used to predict the risk of pathologic fracture, but it remains flawed. We hypothesized that the lesional biologic activity of breast and lung cancer metastases to the proximal femur, as measured by FDG-PET, can supplement Mirels' scoring system to improve surgical decision-making.

Materials and Methods: We retrospectively reviewed records of patients with breast or lung cancer treated between 2005–2013 for metastases to the proximal femur who received FDG-PET scans within the 3 months preceding surgery. We evaluated the association of preoperative fracture with demographic data and FDG standard uptake value (SUV).

**Results:** Nineteen patients (8 lung, 11 breast) with a mean age of 60 years were included. Preoperative fracture occurred in 8. Of 6 patients with a Mirels score  $\leq$ 8, fractures occurred in 4 (66 %), and 3/4 had an SUV  $\geq$ 10. The mean Mirels score was lower for patients with fracture than without (8.4 vs. 9.5, p=0.2). A threshold SUV  $\geq$ 6 had a PPV of 80 %, NPV of 100 %, sensitivity of 100 %, and specificity of 50 %.

**Conclusion:** This study suggests that patients with breast and lung metastases of the proximal femur who have an SUV  $\geq$ 6 should be considered at high risk for pathologic fracture, regardless of Mirels score.

# 2:10 PM. Changes in delayed gadolinium-enhanced MRI of tibiofemoral cartilage (dGEMRIC) indices are not associated with cartilage loss over 1 year: A 3 T MRI study

Michel D. Crema, David J. Hunter, Deborah Burstein, Frank W. Roemer, Ling Li, Nitya Krishnan, Marie-Pierre Hellio Le Graverand, Ali Guermazi. Boston, USA.

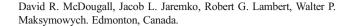
**Purpose:** To assess the associations of baseline dGEMRIC as well as changes in dGEMRIC indices with cartilage loss in the same region of the knee over one year, in a sample of middle-aged women.

Materials and Methods: A total of 140 women (1 knee per subject) aged≥40 years were included. 3.0 T MRI of the knee was performed at baseline and at one year. T2-weighted fat-suppressed sequences (cartilage morphology) and 3D inversion recovery-prepared SPGR sequence 90 min after intravenous gadolinium injection (dGEMRIC) were acquired. The association of any decrease in dGEMRIC indices from baseline to follow-up with cartilage loss in the same region was assessed using logistic regression. We then used the maximal statistical approach to determine at which cut-off value baseline dGEMRIC would be most predictive for cartilage loss.

**Results:** A total of 433 regions were included in the analyses; 25 (5.8 %) had cartilage loss over one year and 408 (92.2 %) did not. No significant associations between change in dGEMRIC indices and cartilage loss were observed. A cut-off value of dGEMRIC predicting cartilage loss could not be established.

**Conclusion:** No significant associations were found between changes in dGEMRIC and cartilage loss in the tibiofemoral compartments over one year.

2:20 PM. Comparative validation of an electronic overlay enhanced target-lesion based methodology (KIMRISS) with the volumetric based MRI Osteoarthritis Knee Score (MOAKS) for scoring bone marrow lesions in the knee in osteoarthritis: Data from the Osteoarthritis Initiative



**Purpose:** We sought to compare the reliability and responsiveness to change of the KIMRISS and MOAKS scoring systems for assessing BML.

Materials and Methods: Data for these analyses are from the OAI public use data set(s). MRI scans were evaluated at enrolment and 1-year follow-up for 80 patients. BML was scored by two readers using MOAKS and KIMRISS. A semitransparent graphic overlay was used with KIMRISS to determine a total volume BML score. Inter-observer reliability of status and change scores was assessed by intra-class correlation coefficient (ICC3, 1), Discrimination was assessed using Guyatt's effect size.

**Results:** Inter-observer reliability of BML (status and change) was higher for KIMRISS (ICC 0.84 and 0.82) than MOAKS (ICC 0.79 and 0.53). KIMRISS change scores showed greater discrimination than MOAKS (Guyatt's 0.59 vs. 0.18).

Conclusion: Direct semi-quantitative assessment of BML on MRI using an electronic overlay with KIMRISS was more sensitive to change in BML than the commonly used MOAKS system, with equivalent or better reliability.

### 2:30 PM. Trajectory of structural tissue damage prior incident radiographic knee osteoarthritis: Long term prediction over 4 years

Frank W. Roemer, C Kent Kwoh, Michael J Hannon, David J Hunter, Robert Boudreau, Felix Eckstein, Tomoko Fujii, Ali Guermazi. Boston, USA.

**Purpose:** To assess if presence and severity of structural OA features over 4 years increase risk for incident radiographic osteoarthritis (ROA).

Materials and Methods: We studied 355 knees from the Osteoarthritis Initiative that developed incident ROA. They were each matched by gender and age with a control knee with the same KL grade at baseline. MRIs were read using the MOAKS scoring system. Conditional logistic regression was applied to assess the risk of incident ROA in regard to presence of bone marrow (BMLs) and cartilage lesions, meniscal damage, Hoffa- and effusion-synovitis at 4 time points prior the case defining visit. Results: None of the features present 4 or 3 years prior predicted incident ROA. 2 years prior only presence of Hoffa-synovitis (OR 2.31[1.19, 4.48]) and medial meniscal damage (OR 2.44[1.13, 5.31]) predicted ROA. One year prior all features but lateral meniscal damage and meniscal extrusion predicted ROA with odds highest for medial tibiofemoral BMLs (OR 6.50[2.27, 18.62].

**Conclusion:** Presence of structural MRI-detected joint damage 3 and 4 years prior incident ROA does not increase risk of ROA. However, one year prior almost all features increased risk of ROA suggesting that the joint status one year prior seems to be most relevant for ROA development.

### 2:40 PM. Osteo-Meniscal Impingement: MRI Findings

Marcelo Bordalo-Rodrigues, Bruno Van de Berg, Paulo Victor Partezan Helito, Conrado Cavalcanti, Frederic Lecouvet, Jacques Malghem, Pascal Poilvache, Gilberto Luís Camanho. Sao Paulo, Brazil.

**Purpose:** Osteo-meniscal impingement is a particular clinico-radiological entity, first described in Europe (2007). It is defined by pain in the medial compartment with the presence of a displaced meniscal fragment causing impingement over the adjacent subchondral bone with consequent focal depression and bone marrow edema. Since this is a little known entity, we sought to describe the MRI findings of patients with osteo-meniscal impingement.

**Method and Materials:** In a retrospective study between January 2010 and January 2012, we reviewed all patients with clinical suspicion of



medial meniscus tear which presented with medial compartment pain. A musculoskeletal radiologist (10 years' experience) analyzed all knee MRI examinations identifying at least two of the previously described osteomeniscal impingement signs: medial meniscus tear with a displaced fragment to the menisco-femoral or menisco-tibial recesses, focal bone depression and adjacent focal bone marrow edema. Arthroscopic records were also evaluated.

**Results:** 24 patients met the imaging criteria for osteo-meniscal impingement (16 men, 8 women, mean age 52,7 years). 21 patients presented an inferior displaced medial meniscus fragment (62 %) and 8 presented a superior meniscal displacement (38 %). Focal bone depression was found in 58 % (14/24) and bone marrow edema in 87.5 % (21/24) of the cases. Arthroscopy was performed in 8 of these 24 cases, with confirmation of a displaced meniscal fragment in all cases.

Conclusion: Our data indicates the osteo-meniscal impingement must be considered in the differential diagnosis of middle-aged patients with medial compartment pain and clinical suspicion of medial meniscus tear and, therefore, radiologists must be aware of the MRI signs of this particular clinico-radiological entity.

### 2:50 PM. The effect of weight bearing on meniscal extrusion

Ryan K L Lee, James F Griffith Joyce H Y Leung. Hong Kong.

**Purpose:** Increasing meniscal extrusion is associated progression of knee osteoarthritis. It was shown recently on MRI, during simulated weight bearing in the supine position that meniscal extrusion significantly increases in the loading position. This is the first study to investigate the effect of true full weight bearing on the severity of meniscal extrusion.

**Materials and Methods:** This is prospective study of 25 symptomatic patients (F:M=13:12, mean age 51.2±14.2 years) with meniscal extrusion initially found on 3.0 T MR imaging (20 medial, 5 lateral menisci) and 25 normal asymptomatic young control subjects (F:M=13:12, mean age 25.0±3.5 years). All patients and controls were examined by 0.25 T MRI (G-Scan, Esaote, Italy) in both the supine and standing positions. Severity of meniscal extrusion was compared between supine and standing positions.

**Results:** For patients with known meniscal extrusion, there was no significant difference in the severity of meniscal extrusion for imaging at 0.25 T and 3.0 T MRI in the supine position (2.3 mm vs. 2.5 mm, p= 0.67). Meniscal extrusion increased significantly between the supine to standing positions (2.3 mm vs. 4.3 mm, p=0.01). All normal controls had no meniscal extrusion in both supine and standing positions.

**Conclusion:** Standing MRI allows appreciation of increasing extrusion in those patients with meniscal extrusion evident in the supine position. This assessment may potentially predict the progression of knee osteoarthritis better than in supine MR imaging. Non-extruded menisci do not extrude during weight bearing.

# 3:00 PM. Comparison of bi-Component T2 relaxation time parameters of menisci in asymptomatic volunteers and patients with osteoarthritis using mcDESPOT

Richard Kijowski, Fang Liu, Alexey Samsonov, John Wilson. Madison, USA.

**Purpose:** To compare bi-component T2 parameters of menisci in asymptomatic volunteers and patients with OA.

**Materials and Methods:** 3D-FSE and mcDESPOT bi-component T2 mapping sequences were performed on the knee of 11 asymptomatic volunteers and 14 patients with OA. T2 of the rapidly and slowly relaxing water components (T2S and T2L) and fraction of the

rapidly relaxing water component (FS) were measured in the medial and lateral menisci and medial and lateral cartilage compartments. 3D-FSE was used to determine BLOK scores and to classify menisci as normal in asymptomatic volunteers (N=22), intact in OA patients (N=20), and torn in OA patients (N=8).

**Results:** Mean values for normal menisci, OA menisci without tear, and OA menisci with tear were 10.3, 11.6, and 12.5 ms for T2S, 30.9, 35.6, and 39.8 ms for T2L, and 0.34, 0.32, and 0.28 for FS with significant differences (p<0.0001) between groups of menisci. There was strong correlation (p<0.001) between menisci T2S, T2L, and FS values and BLOK scores and cartilage T2S, T2L, and FS values within the same knee compartment.

**Conclusion:** OA patients had decreased FS and increased T2S and T2L of menisci than asymptomatic volunteers with greater changes associated with more severe meniscus and cartilage degeneration.

# 3:10 PM. In vivo quantitative ultra-short echo time MR Imaging of temporomandibular joint Disc

Won C. Bae, Sheronda Statum, Kyu-Sung Kwack, Robert Healey Reni Biswas, Christine B Chung. San Diego, USA.

**Purpose:** To compare quantitative ultrashort echo time (UTE) T2\* values of temporomandibular joint (TMJ) discs of normal and symptomatic subjects.

**Material and Methods:** Unilateral TMJ of asymptomatic (n=5, 3F/2M, 37+/-18 years, mean+/-SD) and symptomatic (n=3, 2F/1M, 52+/-9 years) subjects were imaged at 3 T in the sagittal plane using a quantitative UTE T2\* sequence: TR=300 ms, TE=0.01, 1, 3, 8, 11, 35 ms, field of view=80 mm (Fig.1A to C). UTE T2\* value of TMJ discs were determined in a region of interest (Fig.1C, ROI). UTE T2\* values between subjects were compared using ANOVA.

**Results:** Using the UTE T2\* sequence, the TMJ disc (Fig. 1, star) is depicted with a high signal intensity at the shortest TE of 0.01 ms (Fig.1A) and with lowered signal intensity at longer TEs of 3 ms (Fig.1B) and 8 ms (Fig.1C). The mean UTE T2\* values (Fig.1D) of asymptomatic and symptomatic subjects were 7.4+/-1.5 ms and 14.0+/-4.7 ms, respectively, showing a slightly higher (ANOVA p=0.15) but variable values for the symptomatic group.

**Conclusion:** These results show feasibility of in vivo quantitative MR evaluation of TMJ disc using the UTE MR technique, which may provide sensitive and objective measure of TMJ disc degeneration in TMD patients.

# $3{:}20\ PM.$ The iliotibial band in acute knee trauma: Patterns of injury on MR imaging

Ramy Mansour, David McKean, Philip Yoong, James L Teh. Oxford, United Kingdom.

**Purpose:** The appearance of the iliotibial (ITB) band is rarely described in MRI of acute knee trauma. We hypothesize that injury of the ITB is associated with internal derangement, in particular anterior cruciate ligament (ACL) tears and posterolateral corner (PLC) disruption.

Materials and Methods: A retrospective review was completed of 200 MRI scans performed for acute knee trauma. Patients were excluded if there was a history of injury over 4 weeks from the time of the scan. The ITB was scored as normal, minor sprain (Grade 1), severe sprain (Grade 2) and torn (Grade 3). The menisci and ligaments of each knee were also assessed

**Results:** The ITB was injured in 115 cases (57.5 %). Grade 1 injury was seen in 90 cases (45 %), Grade 2 injury in 20 cases



and Grade 3 injury in 5 cases. The ACL was injured in 53.5 % of cases (n=107). There is a significant association between ITB injury and ACL rupture (P<0.05), as well as acute patellar dislocation (P<0.05). There were ten cases of significant PLC injury, and all were associated with ITB injury, including 4 ITB tears. **Conclusion:** ITB injury is relatively common and strongly associated with ACL rupture, PLC injury and patellar dislocation.

### Session 2

Moderators: Miriam Bredella, Boston, USA and Jenny T. Bencardino, New York, USA

3:40 PM. Evaluation of periprosthetic changes in non-Metal on Metal total hip prostheses with and without complications with metal artifact reducing MRI

Gunilla M. Müller, Tord v. Schewelov, Sven Månsson, Markus F. Müller, Björn Lundin. PhD. Malmö, Sweden.

**Purpose:** Evaluation of periprosthetic changes in non Metal on Metal (nonMoM) total hip arthroplasty (THA) with complications using MARS MRI preoperatively and comparison with a matched control group and with operative findings.

**Materials and Methods:** 22 patients with THA, 11 with signs of complications (mean age 73 years) and 11 controls (mean age 63 years) underwent MRI with metal artifact reducing sequences (MARS) on a 1.5-T imager. Two musculoskeletal radiologists analyzed the images regarding periprosthetic changes. Kappa-test was used to analyze reader's agreement and McNemars to compare MRI and operation findings.

**Results:** Osteolysis was present in acetabular bone in 8/11 patients preoperatively and in 4/11 controls, in femoral bone in 6/11 and 4/11 hips, soft tissue mass (STM) in 6/11 and 3/11 hips, respectively. Operatively, 7/8 osteolysis were found in acetabular bone (P=1.0) and 6/6 in femur (P=1.0). Interreader agreement was very good for detecting STM (0.82) and osteolysis in acetabulum (0.82), and moderate for osteolysis in femur (0.61).

Conclusion: MARS allowed to detect all osteolyses but one in acetabular and femoral bone preoperatively. Reader agreement was very good in acetabular bone and STM and moderate for femur. There were more pathologic findings in the patient group compared to controls.

3:50 PM. The prevalence and significance of ultrasound and sonoelastography detected Achilles tendon abnormalities in asymptomatic footballers: A longitudinal study

Chin Chin Ooi, Michal Schneider, Peter Malliaras, David Connell. Singapore, Singapore.

**Purpose:** To identify the prevalence of Achilles tendon sonographic abnormalities in asymptomatic elite footballers and whether they predict end of the season Achilles pain.

Materials and Methods: Using ultrasound and sonoelastography, 84 Achilles tendons (42 footballers) were examined at baseline (preseason) and nine months later (end-season) for the existence of hypoechogenicity, delamination, neovascularization, insertional enthesopathy and/or intratendinous softening. The anteroposterior (AP) thickness and cross-sectional area (CSA) were measured. Players

reporting Achilles pain at the end-season were classified as "symptomatic".

**Results:** Thirty-four percent of the asymptomatic tendons had baseline sonographic abnormalities. Eight Achilles (8/84=9.5 %) of six footballers were symptomatic at the end-season. Baseline AP thickness and CSA were significantly greater in symptomatic footballers at the end-season than asymptomatic footballers (0.55±0.5 cm versus 0.49±0.4 cm, p<0.001, and 0.62±0.6 cm2 versus 0.56±0.6 cm2, p=0.007). The presence of baseline intratendinous softening and delamination were associated with end-season symptoms (p<0.001; p=0.026, respectively). No relationship between other sonographic abnormalities and the development of symptoms was observed.

**Conclusion:** Asymptomatic sonographic abnormalities were relatively common among the footballers. Greater AP thickness and CSA as well as the presence of intratendinous softening and delamination were associated with increased risk of developing symptoms.

# 4:00 PM. Predictive MRI correlates of lesser metatarsophalangeal joint (MPJ) plantar plate (PP) tear

Hilary Umans, Rachel Umans, Benjamin Umans, Elisabeth Elsinger. New York, USA.

**Purpose:** To identify strong predictors of MPJ PP Tear using MRI, since primary signs can be subtle or occult, and misdiagnosis and mistreatment are common.

Materials and Methods: 50 randomized cases (35 female, 15 male, average 52 years) of PP tear and 50 control (41 female, 9 male, average 35 years) noncontrast forefoot MRI (Oct 2012-Jan 2014, 1.5 or 3.0 Tesla) were reviewed, blinded to history, by an MSK radiologist for imaging findings correlated with PP tear. A collaborator performed quantitative measures of metatarsal (MT) axis rotation, 2nd MT protrusion, submetatarsal fat pad thickness and toe rotation. Kappa statistic, t-test, Wilcoxon rank sum test were performed. Classification trees were created to identify combinations of findings that have a strong predictive value for PP tear.

**Results:** There are significant, reproducible differences in measured MT axis rotation and 2nd MT protrusion between PP tear and control groups. Among qualitative findings, pericapsular fibrosis is the most predictive, followed by 2nd toe enthesitis, flexor tendon subluxation, splaying of the 2nd and 3rd toes and lesser MT supination.

**Conclusions:** There are significant, highly reproducible quantitative and qualitative MRI findings associated with lesser MPJ PP tear.

4:10 PM. Diffusion Tensor Imaging, T2 mapping, and various fat suppression imaging in early state of denervated skeletal muscle: Experimental study in rats

Dong-Ho Ha, Sunseob Choi, Kyung Jin Suh. Busan, Korea.

**Purpose:** To simultaneously evaluate the sequential alteration of the diffusion tensor imaging indices, T2 values and subjective signal intensity change on various fat suppression techniques in the early state of denervated skeletal muscle in the rat model.

**Materials and Methods:** Institutional animal use and care committee approval was obtained. Complete neurotmesis of the sciatic nerve of 8 white rats was performed. MR imaging were examined before the surgery and follow up after 3 days, 1 week, and 2 weeks. We measured FA, mADC and T2 values in the gastrocnemius muscle. We also assessed the subjective visual signal intensity changes on chemically selective fat suppression, STIR and IDEAL imaging techniques.

**Results:** After 3 days FA began to decrease significantly  $(0.35\pm0.06, P=0.012)$ . After 1 week and 2 weeks, FA also significantly decreased. T2



values significantly increased after 1 week (38.11 $\pm$ 6.41, P=0.017) and markedly increased after 2 weeks (46.53 $\pm$ 5.17, P=0.012). Three days and 2 weeks studies showed identical change on all fat suppression images. At the 1 week studies, IDEAL imaging showed less prominent change without statistical significance (P=0.256).

**Conclusion:** The FA and T2 values will be effective parameters to observe the early state of denervated muscle.

### 4:20 PM. Is there a role for Diffusion-Weighted MRI (DWI) in the diagnosis of central cartilage tumours?

Hassan Douis, Lee Jeys, Robert Grimer, A. Mark Davies. Birmingham, UK.

**Purpose:** The aims of this study are to assess whether DWI can differentiate; (i) central enchondromas from chondrosarcomas (ii) low-grade from high-grade central cartilage lesions.

Materials and Methods: 52 patients with central cartilage tumours were included. Patients underwent conventional MRI and DWI (b-values 50, 1200s/mm2) with ADC mapping. The slice on MRI with the most aggressive imaging features was identified. The corresponding mean ADC-map of the tumour at this position was measured. Statistical analysis was performed using ANOVA and Student's t-tests.

**Results:** There were 24 enchondromas, 5 atypical cartilaginous lesions, 15 Grade 1, 3 Grade 2, 2 Grade 3 and 3 dedifferentiated chondrosarcomas. Mean ADC-values (x10–6 mm2s–1) for enchondromas, atypical cartilaginous lesions, grade 1 CS, grade 2, CS, grade 3 CS and dedifferentiated CS were 1896, 2048, 2152, 2170, 2076, 1261 respectively. ANOVA-test demonstrated a statistically significant difference in ADC-values in all groups (p=0.001). Post-hoc analysis revealed this was due to difference in ADC-values in dedifferentiated CS. Mean ADC-value in low-grade chondroid lesions was 1999 whilst ADC-values for high-grade chondroid lesions was 1805. This difference was not statistically significant (p=0.16). **Conclusion:** DWI cannot differentiate between enchondromas and chondrosarcomas and does not aid in the distinction of low-grade from high-grade chondroid lesions.

# 4:30 PM. SHINKIE (Nerve-Sheath Signal Increased with Inked Rest-Tissue Rare Imaging)—Novel 3D isotropic MR Neurography technique

Jared Kasper, Avneesh Chhabra. Dallas, USA.

**Purpose:** Evaluate relative merits of SHINKIE over conventional 3DIRTSE for LS plexus MRN.

Materials and Methods: Prospectively acquired 21 consecutive LS MRN exams on 3 Tesla scanner using both 1.5 mm isotropic 3DIRTSE and SHINKIE techniques. Two trained observers evaluated all images for motion and pulsation artifacts, nerve signal to noise (SNR), contrast to noise (CNR), nerve—fat ratio, quality as well as degree of fat suppression (muscle—fat ratio) and depiction of LS plexus.

Results: 4 exams were excluded due to prior spine surgery. Bowel motion artifacts, pulsation artifacts, inhomogeneous fat saturation and patient motion were seen in 16/17, 0/17, 17/17, 2/17 in 3DIRTSE and 0/17, 0/17, 0/17, 1/17 in SHINKIE, respectively. The p values were significant in SHINKIE for nerve SNR (<0.01), CNR (<0.01), nerve to fat (<0.01) and degree of fat saturation, muscle to fat ratio (p<0.01). Both 3D IRTSE and SHINKIE showed all LS plexus nerve roots, sciatic and femoral nerves universally. Smaller branches including obturator nerves, ilioinguinal and iliohypogastric were seen in 10/17, 5/17, 1/17 in 3DIRTSE and 17/17, 16/17, 7/17 in SHINKIE exams, respectively.

**Conclusion:** In addition to the benefit of effective vascular signal suppression, the SHINKIE MRN technique demonstrates increased conspicuity of smaller LS plexus branches.

4:40 PM. Ulnar groove position of the extensor carpi ulnaris tendon (ECU) on MRI of asymptomatic volunteers in forearm pronation, neutral and supination

Seema Meraj, Nidhi Jain, Catherine N. Petchprapa. New York, USA.

**Purpose:** To evaluate ECU tendon position in forearm pronation, neutral and supination in asymptomatic volunteers.

**Materials and Methods:** Axial proton density-weighted MR imaging through the distal radioulnar joint with the forearm prone, neutral and supine was performed on 18 asymptomatic wrists. The percentage of the tendon located beyond the ulnar-most border of the groove was recorded (0 %, 1–50 %, 51–99 %, 100 %/ dislocated).

**Results:** All volunteers (6 men, 3 women; mean age 29.78 years; range 27–32) were asymptomatic; there was no history of ulnar side pain/snapping, prior trauma, or surgery. Only 1/18 ECU remained within the groove throughout pronation, neutral, and supination. In 16/18, the ECU translated ulnarly from pronation to supination. The tendon dislocated in 0/18 prone, 4/18 neutral, 9/18 supine. In 3/18 prone, 0/18 neutral, and 2/18 supine wrists, the tendon was 51–99 % beyond the ulnar border of the ulnar groove; 2/5 of these subluxed >75 %.

Conclusion: The ECU is known to shift in an ulnar direction in forearm supination; however the degree of tendon translation has not been previously documented on normal wrist MRIs. The ECU was noted to significantly ulnar sublux/dislocate in the majority of our asymptomatic volunteer population in supination.

### 4:50 PM. The effect of automatic exposure control on radiation dose

Sayed Ali, Erin Crane, Alex Lambi, Steven Popoff, Summer Kaplan. Philadelphia, USA.

**Purpose:** To assess the dose to abdominal structures with or without gonad shielding and AEC (automatic exposure control), in order to optimize a low dose protocol for pelvic radiography.

Materials and Methods: 4 MOSFET dosimeters were implanted in a cadaver at 4 locations. Radiography was performed using AEC or manual settings. Doses were log-transformed then analyzed using two-sample t-tests. All results were confirmed with nonparametric Wilcoxon-Mann–Whitney Exact tests. Significance was set at 0.05.

**Results:** AEC settings without a gonad shield were 80 kVp, 14 mAs, with average doses<5 cGy. With a shield, AEC settings were 80 kVp, 102 mAs, with doses under the shield<3 cGy and outside the shield 23–39 cGy. The increased dose outside the shield was significant (p<0.001). Manual settings resulted in an average 11.2 cGy dose outside the shield and negligible dose under it.

**Conclusion:** AEC without gonad shielding gives the lowest average dose across all 4 points assessed. Manual techniques with shielding results in a 240 % increase in dose outside the shield. Gonad shielding with AEC results in high doses at all points. Our results suggest dose to radiosensitive organs is best optimized by AEC without gonad shielding.

### 5:00 PM. SSR Award Paper

3D morphologic assessment of normal and abnormal SI joints and the potential implications in the development of pain syndrome



Mary Kristen Jesse. Denver, USA.

**Purpose:** Better understand normal sacroiliac joint morphology through the utilization of 3D surface rendered imaging of the SI joint and investigate morphologic trends in SI pain syndrome patients.

Materials and Methods: 3D surface rendered images of the SI joint were acquired in 223 normal controls. Morphologic 3D assessment of the articular surface morphology and measurements of sacral tilt, inclination and sacral and iliac surface area were performed. SI joint morphologies were further classified into three types based on shape (Types 1, 2 and 3). Thirty-four pain patients were analyzed in a similar fashion as above with emphasis on SI articular surface area and surface morphology.

**Results:** Average sacral tilt, inclination and surface areas were established in the control group. Visual morphologic assessment revealed a dominance of the Type 2 morphologic variant. Significant association was found between Type 3 morphology and the development of pain (p-value 0.04) and lower mid and caudal inclination and the development of pain (p-values 0.01 and 0.049).

**Conclusion:** Our study provides a new look at SI joint morphology with insight into visual morphologic differences in articular surface shape and variability in articular surface area and determines an association between morphology and the development of pain.

### 5:10 PM. AMS Award Paper

Pre- and postoperative Diffusion Tensor Imaging and fiber tractography in cervical spondylotic myelopathy: Short-term preliminary results

Eugene Lee, MD1, Joon Woo Lee, MD, PhD1, Guen Young Lee, MD, PhD1, Heung Sik Kang, MD, PhD1. Seoul, Korea

**Purpose:** To investigate the value of pre- and postoperative DTI parameters in addressing the preoperative severity of cervical spondylotic myelopathy (CSM) and predicting short-term outcomes following surgery.

Materials and Methods: Twenty patients who underwent surgical decompression due to CSM were retrospectively enrolled. DT 3.0-T MR images with fiber tractography were obtained before and one-month after surgery. DTI parameters and patterns of fiber tractography were related to clinical severity and outcome of surgery based on mJOA scores.

**Results:** Mean FA and ADC values from C2-7 were correlated with preand postoperative mJOA scores. Neurologic recovery was demonstrated by improvement of mJOA scores ( $12.7\pm3.2$  vs.  $15.3\pm2.3$ ; p=0.0004), however none of the DTI parameters showed statistically significant improved value. Preoperative fiber tractography were associated with clinical disease severity (r=-0.583, p=0.029), but postoperative fiber tractography were not. ROC analysis showed that any of DTI or clinical parameters was not significant predictable factor for good surgical outcome. There were six patients (30%) of failed fiber tracking on postoperative DTI. Posterior instrumentation was possible factor for failed fiber tractography.

**Conclusion:** DTI is useful diagnostic method for assessing the preoperative disease severity. However, the utility of postoperative DTI should be further investigated.

5:20 PM. ESSR Award Paper Not available at the time of submission.

Breakout Scientific Poster Session ISS—Members Meeting Wednesday October 15th, 2014, 12:30 PM—1:30 PM



Ad Hoc Scientific Session Committee:

Miriam Bredella, Juerg Hodler, Carrie Inwards, Christian Pfirrmann, Kathryn Stevens, Martin Torriani. Chair: Jenny T. Bencardino.

### Session 1: Focus on Tumors 12:30-1:00 PM

**Moderators:** Kathryn Stevens, Stanford, USA and Christian Pfirrmann, Zurich, Switzerland

12:30 PM. Differentiation of acute benign and malignant vertebral body fractures with quantitative diffusion-weighted MRI: effect of ROI size and positioning on interobserver variability, sensitivity and specificity

Tobias Geith, Margarita Braunagl, Mike Notohamiprodjo, Andreas Biffar, Gerwin Schmidt, Hans-Roland Dürr Steven Sourbron, Maximilian Reiser, Andrea Baur-Melnyk. Munich, Germany.

**Purpose:** To evaluate the effect of different sizes and positioning of regions of interest (ROIs) on the inter-observer variability, sensitivity and specificity in differentiating acute benign and malignant vertebral body fractures with quantitative diffusion-weightedMRI.

Materials and Methods: 26 acute benign (31.5–86.2 years) and 20 malignant vertebral fractures (24.7–86.4 years) were evaluated. Standard sequences and a diffusion-weighted single-shot turbospin-echo-sequence at different b-values (100,250,400,600 s/mm²) were acquired at 1.5 T. Two readers independently evaluated ADCs of the fractured vertebrae based on regions of interest(ROIs), manually adapted to the whole extension of hyperintense areas on STIR, to the whole outer shape of the fractured vertebrae, and to small spots within each hyperintense area on STIR. Significant differences were determined with Student's t-test. ROC analysis was used to determine sensitivity and specificity. Interobserver correlation was tested with the ICC.

**Results:** ICC was high for all ROI-sizes (ICC=0, 80-096). Highest AUC (0.803) was found for the ROIs on the whole outer vertebral contour (sensitivity=68%, specificity=88%). ROIs exactly adapted to the extension of high signal on STIR had the highest sensitivity (74 %) at a specificity of 83 % (ADC malignant<1,  $48 \times 10$ -3 mm2/s).

**Conclusion:** ROIs exactly adapted to the extension of bone-marrow edema (hyperintense on STIR) provide the highest sensitivity to differentiate acute benign and malignant vertebral body fractures and should be used in quantitative diffusion-weighted MRI.

12:35 PM. The clinical relevance of ADC value of metastatic bone lesions on diffusion weighted MR image: Differences according to the primary tumor, targeted bones, and clinical factors

Ji Seon Park, Min Jae Cha, Young Cheol Yoon. Seoul, Republic of Korea.

**Purpose:** This study is to evaluate whether apparent diffusion coefficient (ADC) value of metastatic bone lesions on diffusion-weighted magnetic resonance (MR) image differs according to the primary cancer, affected bones, and clinical factors, and thus, to determine the clinical relevance of ADC value in patients with bone metastasis.

**Materials and** Methods: This retrospective study was approved by our institutional review board and written informed consents were waived. Two radiologists retrospectively reviewed MR imaging including ADC maps of 67 patients (M: F=38:29, median age, 48 years) who were histologically or clinically diagnosed with bone metastasis. The primary tumors are 29 lung adenocarcinomas, 15 breast carcinomas, 13 HCCs, 6

prostatic carcinomas, and 4 renal cell carcinomas. ADC value of the metastatic tumor regions were compared according to the primary malignancy, affected bones, age and sex by using Kruskal-Wallis test, one-way analysis of variance, Wilcoxon rank sum test and Spearman correlation analysis, with Bonferroni correction. In addition, 38 pre-contrast CT images among 67 patients were also reviewed, and sub analysis between CT density and ADC value was performed.

**Results:** Mean ADC value of the metastatic bone lesions did not show significant difference according to the primary malignancy, affected bones, and clinical variances including age and sex (p>1) in all of the analysis). There was no demonstrable correlation between ADC value and CT density, either (p=0.24). Standard deviation of ADC values of long bone metastasis was larger than that of irregular bone (p<0.01). Intra- and interobserver agreement of mean ADC values are excellent (p=0.981) and (p=0.981), respectively).

**Conclusion:** Assessment of ADC values of metastatic bone lesions is not reliable for differentiation of primary cancer type.

## 12:40 PM. Total en-bloc spondylectomy for the management of primary and metastatic spine tumors

Addisu Mesfin, Mostafa El-Dafrawy, Johnny U.V Monu, Khaled Kebaish. Rochester, USA.

**Purpose:** Total en-bloc spondylectomy (TES) is indicated for en-bloc resection of malignant or primary spine lesions. Our objective is to report the surgical and clinical outcomes of spinal lesions managed via TES.

Materials and Methods: Ten patients underwent TES from 2001 through 2013 at a single institution. We collected their demographics, surgical outcomes (e.g., estimated blood loss, complications), and clinical outcomes (recurrence, survival). All patients presented with pain and were American Spinal Injury Association (ASIA) grade E. Anterior column reconstruction was performed using allograft (seven patients), Mesh cage (two patients), and polymethylmethacrylate (one patient). An average of 2.3 (2–4) of 6 portions of the vertebrae were involved per the Kostuik classification.

Results: Average age was 50.7 years (42–68) and 9 males and 1 female. Eight lesions were in the thoracic spine and 2 were in the lumbar spine. The mean estimated blood loss, operative time, and hospital stay were 3.5 L, 500 min, and 7.8 days. Perioperative complications were pleural tear (two) and one each of the following: aortic tear, vena cava tear, retained sponge, pulmonary embolism, urinary tract infection, pneumothorax, anterior column support failure, and prominent instrumentation requiring removal. Postoperatively, all patients remained ASIA grade E. Two patients had recurrence at distant spinal segments and one had a new lesion in the thigh. Five patients died (mean, 34.5 months post-surgery) and five are alive at mean of 19.6 months post-surgery (6–48).

**Conclusion:** TES is challenging but can be used, in appropriately selected patients, to safely address spinal lesions.

## 12:45 PM. Non-neoplastic tumour-like lesions in the upper limb: incidence and imaging findings at a musculoskeletal referral centre

Ian Pressney, Rikin Hargunani, Michael Khoo, Asif Saifuddin. Stanmore, UK.

**Purpose:** Tumour-like lesions in the musculoskeletal system are not infrequently encountered by the radiologist and represent a diagnostic challenge. The aim of the study was to evaluate the incidence, location and imaging features of non-neoplastic tumour-like lesions of bone and soft tissue in the upper limb.

Materials and Methods: Referrals to our tertiary musculoskeletal oncology centre with a tentative diagnosis of bone or soft tissue malignancy over a 2 year period from March 2007 were assessed. All upper limb non-neoplastic diagnoses were included in the study including both biopsy proven and imaging suggested diagnoses.

**Results:** A total of 2,432 consecutive cases were identified with 496 (20.4 %) cases diagnosed as non-neoplastic with 108 (21.8 %) within the upper limb. Fifty-three of 108 (49.1 %) were biopsy proven versus 55 diagnoses from imaging alone. The most frequent diagnoses included bursitis/synovitis/ tenosynovitis (16), CRMO/ SAPHO (15), osteomyelitis (9), abscess (7), and haematoma (6).

**Conclusion:** Tumour-like lesions are relatively common representing one fifth of all referrals to a tertiary centre with one fifth of these within the upper limb. The radiologist needs to be acutely aware of the possibility of non-neoplastic diagnoses and their potential imaging findings.

### 12:50 PM. Tumors of the foot: a single institution experience

Pietro Ruggieri, Elisa Pala, Teresa Calabrò, Giulia Trovarelli, Andrea Angelini, Giuseppe Rossi, Eugenio Rimondi. Bologna, Italy.

**Purpose:** Tumors of the foot are rare. This epidemiologic study evaluated incidence, histology and treatment strategy of most common tumors of the foot

**Material and Methods:** 1.170 tumors of the foot were retrospectively analyzed. Imaging Included radiographs in all patients, and CT and MRI when available.

Results: There were 189 soft tissue and 981 bone lesions. Benign or pseudotumoral lesions were 870 (74 %): multiple chondromas (168), osteoid osteoma (164), solitary osteochondroma (47), Nora disease or similar reactive lesions (78), calcaneus cyst (51), aneurysmal bone cyst (45) are the most frequent lesions observed. Malignant lesions were 300 (26 %): Ewing's sarcoma (44), central chondrosarcomas (29), metastatic carcinoma (24) and other more rare entities. Localizations were phalanges (240; 20 %), metatarsal region (245; 21 %) and hind foot (685; 59 %). Soft tissue lesions included villonodular synovitis (20), lipoma (19) and schwannoma (13) as most frequent benign and synovial sarcoma (55) among malignancies. Benign and pseudotumoral lesions were generally treated with curettage. Chemotherapy and surgery was required for high grade malignant lesions. Amputation may be required for tumors involving the hind foot.

**Conclusions:** Malignant tumors are relatively rare, but a high level of attention on imaging and clinical features is required. In every doubtful case, a biopsy should be done.

12:55-1:00 PM. Discussion

### Session 2: Miscellaneous 1:00-1:30 PM

**Moderators:** Kathryn Stevens, Stanford, USA and Christian Pfirrmann, Zurich, Switzerland

# $1\!:\!00$ PM. Mobile texting devices: the effect on serum and MRI biomarkers

Sayed Ali, Judith Gold, Feroze Mohamed, Summer Kaplan, Mary Barbe. Philadelphia, USA.

**Purpose:** To determine if serum biochemical and MRI biomarkers differed between high and low volume texters.

**Materials and Methods:** Ten females with a mean age of 20 were recruited, high volume ( $\geq$ 230 texts sent/day; n=5) and low volume ( $\leq$ 25 texts sent/day; n=5)). We examined serum for 20 biomarkers, including biomarkers for inflammation and repair (TNF-R1, IL1-R1 and TGFB1).



We assessed for tendinosis and tenosynovitis, and quantitative characteristics of tendon volume and MRI mean intratendinous signal intensity (MISI) of the thumb tendons. Correlation between serum biomarker concentrations and MISI in the tendons was assessed with a Spearman rank correlation coefficient. A p-value less than or equal to 0.05 was regarded as statistically significant.

**Results:** Three high volume texters had MRI findings of tendinopathy, as did one low volume texter. Increased serum TNF-R1 was found in high volume texters compared to low volume texters, as were non-significant increases in MISI in two thumb tendons. Serum TNF-R1, IL1-R1 and TNF- $\alpha$  showed statistically significant correlation with MISI in these tendons.

**Conclusion:** Serum and MRI biomarkers differed between high and low volume texters, and early onset tendinopathy with concurrent local and systemic inflammation is likely occurring in prolific texters.

# 1:05 PM. Acute hamstring injury in soccer players: distribution of locations and association between location and extent of injury—a large single-center MRI report

Michel D. Crema, Ali Guermazi, Johannes Tol, Jingbo Niu, Bruce Hamilton, Frank W. Roemer.

**Purpose:** To describe in detail the anatomic locations of acute hamstring injuries in soccer players and to assess the relationship between location and extent of edema and tears, based on findings from MRI.

**Materials and Methods:** We included 275 consecutive male soccer players who had sustained acute hamstring injuries. Lesions were recorded in specific locations of the muscles and the largest cross-sectional area of edema and/or tears was assessed in addition. The average value of edema and tears for each muscle was used as the reference standard. The relationships between locations and extent of edema and tears were assessed using one-sample t-test, with significance set at p < 0.05.

**Results:** The long head of biceps femoris (LHBF) was the most commonly affected muscle (56.5 %). Injuries were most common in the myotendinous junction (MTJ) and in proximal locations. The proximal MTJ was associated with a greater extent of edema in the LHBF and semitendinosus muscles (p<0.05). Proximal locations in the LHBF had larger edema (p<0.05). Distal locations in the semitendinosus muscle had larger tears (p<0.05).

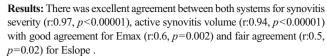
**Conclusion:** The proximal MTJ and proximal locations were more commonly affected and were associated with a greater extent of edema. Distal locations, however, seem to be associated with larger tears.

# $1:\!10~PM.$ Determination of synovial activity of the wrist in rheumatoid arthritis (RA): Low field (0.25 T) versus high-field (3.0 T) MRI

Ryan K L Lee, James F Griffith, Joyce H Y Leung, DF Wang, Lin Shi, Edmund Li, L S Tam Hong Kong.

**Purpose:** Semiquantitive assessment of synovial activity (RAMRIS score), quantitative assessment of enhancing synovial volume (ml3) and the degree of synovial perfusion are all used to determine disease activity and response to treatment in RA. This is the first study to compare assessment of these three indices between low field (0.25 T) and high field (3.0 T) MRI in RA patients.

**Materials and Methods:** Prospective study of 21 patients (F:M=16:5, age 50.0±9.8 years) with active RA. Dynamic contrast-enhanced MRI of the most severely affected wrist was performed on both 0.25 T (G-SCAN, Esaote, Italy) and 3.0 T systems. Three MRI parameters [synovitis severity), active synovial volume, and synovial perfusion indices (maximum enhancement Emax (%,) enhancement slope Eslope (%/sec))] were independently compared for low-field and high-field MR systems.



**Conclusion:** 0.25 T MRI yields excellent assessment of synovitis, synovial volume and fair to good assessment of perfusion parameters. It can be used to assess disease activity and therapeutic response in RA patients.

# 1:15 PM. Comparison of metal related artifacts by application of metal artifact reduction software or not in gemstone spectral imaging dual energy CT

Hyun-joo Kim, Jang Gyu Cha, Sung Tae Park, Seong Sook Hong, Jung Hwa Hwang. Seoul, Korea.

**Purpose:** To know the effectiveness of gemstone spectral imaging (GSI) dual-energy CT (DECT) with/without application of metal artifact reduction software (MARs) in different keV values.

Materials and Methods: Total 25 patients who received spine surgery with metallic devices underwent GSI-DECT. The CTs were performed using fast kV-switching between 80 and 140 kV. The CT data were reconstructed with monochromatic energy in the range 70–140 keV with/without MARs. All images were retrospectively reviewed according to the visibility of periprosthetic regions (bone/soft tissue) by a sixpoint scale (0–5) and the severity of beam-hardening artifacts by using a four-point scale (0–3). Also the size differences of metal devices were measured with or without MARS in the range of 110 keV.

**Results:** The mean age was 58.2. Twelve were male and the others are female. The mean visibility scale of soft tissues is 1.36–3.16 without/ without MARs. That of bones is 1.44–3.8. The mean artifacts scale is 1.92–3 (p-values:<0.0001-1.000). The bone is most effectively visualized in 110 keV and the soft tissue is in 120 keV without MARs. The size of devices measured 1.5 mm smaller and 1.7 mm larger with/without MARs. **Conclusion:** Monochromatic energy image with 110–120 keV without MARs reduced artifacts most effectively.

1:20. Ultrasound-guided fusion imaging-assisted facet joint injections:

Giulio Ferrero, Luca Maria Sconfienza, Emanuele Fabbro, Davide

Orlandi, Pietro Caruso, Enzo Silvestri. Genova, Italy.

preliminary experience

**Purpose:** To increase safety, target accuracy, and efficacy of US-guided facet joint injections using a MR/CT GPS-driven fusion system.

**Materials and Methods:** We evaluated 20 patients (10 males, mean age 65 years, range 56–78 years) with a clinical diagnosis of low back pain and previously investigated with CT (*n*=11) or MRI (*n*=9) in order to confirm the presence of facet joints degenerative changes. All patients received facet joints injection of steroid and anesthetic (0,5 ml triamcinolone acetonide 40 mg/ml+0,5 ml lidocaine 2 % for each joint) of the affected levels under US guidance (Logiq E9, GE healthcare, USA) coupled with a GPS-driven fusion system using MR or CT images. Patients' pain were recorded at 0, 2, 8, 24 weeks using a visual analogue scale (VAS). Wilcoxon statistics were used.

**Results:** No complications were encountered. Facet joint injection was performed in all cases. VAS scale significantly decreased from  $7.3\pm2.7$  (mean $\pm$ SD) at baseline to  $3.2\pm2.7$  at 24 weeks (P<0.01).

**Conclusion:** US needle guidance with MR or CT fusion assistance allows for safe and effective injection of degenerative facet joint disease. This technique may be readily translated also to other applications in which spinal needles are used.

